Graphical Abstract

Selective Filtration of NMR Signals Arising from Weakly- and Strongly-Coupled Spin Systems

Jiaqi Lu, Alexej Jerschow, David E. Korenchan

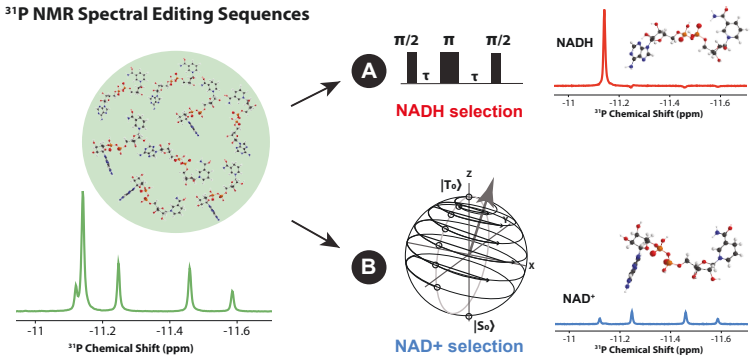

NMR spectroscopy unveils chemical and biological mysteries, but overlapping signals hinder species identification. We introduce spectral editing sequences exploiting nuclear spin interactions in weakly- and strongly-coupled systems. These sequences suppress unwanted magnetization while preserving desired signals. Using a ^{31}P filtration method on a nicotinamide dinucleotide (NAD) model, encompassing NAD^+ and NADH forms, we demonstrate the robustness, versatility, and fidelity of our approach. Our sequences untangle NMR complexities, enabling clearer analysis of complex systems.

Highlights

Selective Filtration of NMR Signals Arising from Weakly- and Strongly-Coupled Spin Systems

Jiaqi Lu, Alexej Jerschow, David E. Korenchan

- MR spectral editing with z-filter for spin resonance elimination, inspired by NMR singlet states.
- The technique overcomes signal-to-noise ratio, scanner stability and field inhomogeneity issues in spectral editing.
- J-synchronized echo train removes strongly coupled resonances for precise editing.
- Effective application on NAD^+ and NADH in a biologically relevant model system.
- Robust editing sequences resistant to shim and pulse offset frequency variations.

Selective Filtration of NMR Signals Arising from Weakly- and Strongly-Coupled Spin Systems

Jiaqi Lu[a], Alexej Jerschow[a], David E. Korenchan[a,b]

[a] *Department of Chemistry, New York University, 100 Washington Square East, Room 710, New York, 10003, NY, USA*
[b] *Department of Radiology, Athinoula A. Martinos Center for Biomedical Imaging, Massachusetts General Hospital, 75 3rd Ave., Room 1400A, Charlestown, 02129, MA, USA*

Abstract

Nuclear magnetic resonance (NMR) spectroscopy is a powerful technique for analyzing chemical and biological systems. However, in complex solutions with similar molecular components, NMR signals can overlap, making it challenging to distinguish and quantify individual species. In this paper, we introduce new spectral editing sequences that exploit the differences in nuclear spin interactions (J-couplings) between weakly- and strongly-coupled two-spin systems. These sequences selectively attenuate or nullify undesired spin magnetization while preserving the desired signals, resulting in simplified NMR spectra or single-species images. We demonstrate the effectiveness of our approach using a ^{31}P spectral filtration method on a model system of nicotinamide dinucleotide (NAD), which exists in oxidized (NAD^+) and reduced (NADH) forms. The presented sequences are robust to field inhomogeneity, do not require additional sub-spectra, and retain a significant portion of the original signal.

Keywords: NMR spectroscopy, Spectral editing, Singlet order, NAD

1. Introduction

Nuclear magnetic resonance (NMR) spectroscopy offers exceptional specificity in distinguishing and quantifying molecular components of liquid or semisolid chemical and biological systems. In complex solutions containing multiple compounds with high structural similarity, however, NMR signals tend to overlap with one another, especially for nuclei with a small range of chemical shift dispersion, such as ^{1}H or ^{31}P. Resolving chemical species from one another in such systems requires leveraging additional nuclear spin properties besides chemical shift. Perhaps the most straightforward approach involves a 2D or higher-dimensional NMR acquisition, in which the indirect acquisition dimensions capture homo- or heteronuclear spin polarization exchange through dipolar couplings (NOESY, ROESY), scalar J-couplings (COSY, TOCSY, HSQC, HMBC, HMQC), or exchange (EXSY) and thereby differentiate spins at similar chemical shifts via the appearance of NMR cross-peaks [1, 2]. Acquiring higher-dimensional data typically requires longer measurement times, however, and a more rapid approach may be desired, especially in low-stability or biological samples where time is of the essence.

Email address: dkorenchan@mgh.harvard.edu (David E. Korenchan)

NMR spectral editing represents a myriad of techniques in which certain NMR peaks are attenuated or nullified while others are preserved, resulting in a simplified one-dimensional NMR spectrum or single-species image. *A priori* knowledge of unique spin properties, such as spin-lattice (T_1) or spin-spin (T_2) relaxation rate constants and scalar couplings, is implemented to tune pulse sequence parameters towards the desired spectral profile. Perhaps the most basic spectral editing sequence is the Carr-Purcell-Meiboom-Gill (CPMG) train of refocusing pulses, which attenuates short-T_2 resonances and improves the spectral baseline [3, 4]. Similarly, signals of a known T_1 relaxation rate can be reduced by choosing an appropriate delay following an inversion pulse, as is used for the fluid-attenuated inversion-recovery (FLAIR) imaging sequence [5] and as has been demonstrated to null lipid or N-acetyl aspartate (NAA) signals for NAA quantification *via* ^{1}H NMR spectroscopy in the brain [6]. Even greater spin selectivity is achieved by harnessing J-couplings, such as with J-difference spectroscopy, J-resolved spectroscopy, or multiple-quantum filtration (MQF) [7, 8]. J-difference spectroscopy alternates selective and broadband refocusing pulses to refocus or not refocus, respectively, a desired J-coupling between two sub-acquisitions. The resulting spectra are added or subtracted from one another to remove or isolate, respectively, the targeted J-coupled spins. ^{1}H J-difference NMR spectroscopy has been implemented *in vivo* to measure lactate, γ-aminobutyric acid (GABA), glutathione (GSH), 2-hydroxyglutarate (2HG), and other metabolites, and MQF approaches can be used to eliminate singlet resonances of uncoupled spins [8]. Recently, both selective J-refocusing and double-quantum filtration have been combined together, along with other filter sequences, to form the Designed Refocused Excitation And optional Mixing for Targets *In vivo* and Mixture Elucidation (DREAMTIME) sequence, which can selectively isolate signals from many spectral components simultaneously [9]. With the advent of *para*-hydrogen induced polarization (PHIP) techniques, it has become possible to selectively enhance ^{1}H signals, then filter out non-enhanced background resonances using the Only Para-Hydrogen Spectroscopy (OPSY) pulse sequence, which leverages the unique spin states created by *para*-hydrogen enhancement to differentiate between signals [10, 11, 12, 13].

However, these techniques have drawbacks. PHIP methodology requires sophisticated equipment that may not be accessible or applicable to *in vivo* ^{1}H spectroscopy. J-difference spectroscopy is susceptible to poor shimming and sample and hardware instability, since the selective pulses employed are sensitive to inhomogeneity in the main magnetic field (B_0), and disturbances between summed or subtracted spectra will distort the final spectrum [8]. These may not be major considerations for typical solution-state NMR, but more complex samples or living subjects often present these problems. MQF in its turn is limited in signal-to-noise ratio because the signal magnitude decreases exponentially with the number of spins involved in the selected coupling network [14]. Spectral editing would therefore benefit from a method that preserves more signal and is robust to field inhomogeneity and instability.

In this work, we present new spectral editing sequences which utilize differences in J-evolution between weakly- and strongly-coupled two-spin systems with overlapping spectral peaks. The fundamental schematic of the approach is shown in Fig. 1. Each pulse sequence places the undesired spin magnetization perpendicular to that of the desired spins. A z-filter [15] utilizing a 90° tip-back pulse with an appropriate phase returns the desired spin magnetization to the z-axis so that undesired magnetization components can then be spoiled by a gradient. We demonstrate that removal of either the weakly-coupled or strongly-coupled

spin pair from the final spectrum is possible by testing our ^{31}P spectral filtration method on a model system of nicotinamide dinucleotide (NAD), both oxidized (NAD^+) and reduced (NADH) forms. The ratio of the two NAD redox states (NAD^+/NADH) is of considerable biological interest because it reflects the overall cellular metabolic state [16]; therefore, several *in vivo* ^{31}P NMR studies and spectral editing approaches have been reported in order to measure this ratio [17, 18, 19]. The sequences presented are robust to B_0 inhomogeneity, do not require adding or subtracting sub-spectra, and preserve a large proportion of the original signal. This technique may be applicable to other molecular systems to simplify NMR spectra and quantify desired chemical species by providing selectivity based on the coupling regime.

2. Theory

In cases where chemical shift does not provide sufficient spectral resolution, it may be possible to distinguish between spin systems by their evolution under different J-couplings, especially if the compounds fall within opposite coupling regimes. The coupling regime of two homonuclear spins I and S depends on the relative magnitudes of the homonuclear scalar coupling J_{IS} and the resonance frequency difference between them, given by a chemical shift difference, $\Delta\delta_{IS}$ (here represented in units of Hertz). In the weakly-coupled regime, $\Delta\delta_{IS} \gg J_{IS}$, and therefore the J-coupling Hamiltonian can be simplified to $H_{J_{IS}} = 2\pi J_{IS}(I \cdot S) \approx 2\pi J_{IS} I_z S_z$ using the secular approximation. In this form, the Hamiltonian satisfies a cyclic commutation relationship with the operators I_x and $2I_yS_z$:

$$[I_x, 2I_zS_z] = -i2I_yS_z$$

A similar cyclic commutation relationship holds between the Hamiltonian, I_y, and $-2I_xS_z$, as well as among the corresponding S-spin operators in the xy-plane. The density matrices $\rho_I(t)$ for spin I and $\rho_S(t)$ for spin S would thus evolve under $H_{J_{IS}}$ following a 90_y° excitation as:

$$\rho_I(t) = I_x\cos(\pi J_{IS}t) + 2I_yS_z\sin(\pi J_{IS}t) \quad (1)$$

$$\rho_S(t) = S_x\cos(\pi J_{IS}t) + 2I_zS_y\sin(\pi J_{IS}t) \quad (2)$$

In contrast, a strongly-coupled homonuclear spin system AB, where $\Delta\delta_{AB} \ll J_{AB}$, will evolve differently under $H_{J_{AB}}$ after the same 90_y° excitation because the secular approximation to the Hamiltonian is no longer valid. This results in a more complex mathematical expression. Neglecting chemical shift evolution (such as in the case of a spin echo of total time t), the density matrix $\rho_{AB}(t)$ has been previously estimated by Nakai and Mcdowell to be (adapted from Eqs. (6) and (14-16) from reference [20]):

$$\rho_{AB}(t) \approx f(t)(A_x + B_x) + g(t)(2A_yB_z + 2A_zB_y)$$

where

$$f(t) = p(t)\cos(\pi J_{AB}t) - q(t)\sin(\pi J_{AB}t)$$

$$g(t) = p(t)\sin(\pi J_{AB}t) + q(t)\cos(\pi J_{AB}t)$$

$$p(t) = \sin^2(\theta_{AB}) + \cos^2(\theta_{AB})\cos\left(\frac{\Omega_{AB}}{2}t\right)$$

$$q(t) = \cos(\theta_{AB})\sin\left(\frac{\Omega_{AB}}{2}t\right)$$

and

$$\theta_{AB} = \arctan\left(\frac{\Delta\delta_{AB}}{J_{AB}}\right) \tag{3}$$

$$\Omega_{AB} = 2\pi\sqrt{J_{AB}^2 + \Delta\delta_{AB}^2} \tag{4}$$

The spin system parameter θ_{AB} in Eq. (3) is often called the "mixing angle" and describes how strongly coupled the AB spin system is, with smaller mixing angles corresponding with more strongly coupled spin systems. The equations above demonstrate that an AB spin system will evolve less and less significantly away from the rank-1 order-1 product operators $(A_x + B_x)$ the more strongly coupled it is. For example, if $J_{AB} = 4\Delta\delta_{AB}$ ($\theta_{AB} \approx 14°$), then the $(A_x + B_x)$ operators do not decrease below 88.2% of their maximal expectation values, based upon the expression for $p(t)$ above. In this case, it may be appropriate to make the approximation $\rho_{AB}(t) \approx A_x + B_x$.

If one therefore wished to selectively suppress the IS spin system while keeping signals from an AB system, one could excite all spins with a broadband $90_y°$ pulse, then allow the IS spin system to evolve under $H_{J_{IS}}$ for a time $t = \frac{1}{2J_{IS}}$, followed by tip-back to the z-axis and gradient spoiling (these two last steps are known as a z-filter [15]):

$$I_z + S_z + A_z + B_z \xrightarrow{90_y°} I_x + S_x + A_x + B_x \xrightarrow{H_{J_{IS}}, t=\frac{1}{2J_{IS}}} 2I_yS_z + 2I_zS_y + A_x + B_x$$

$$\xrightarrow{90_{-y}°} -2I_yS_x - 2I_xS_y + A_z + B_z \xrightarrow{\text{spoil}} A_z + B_z$$

One could then apply an excitation pulse and detect the AB spin system resonances. Note that any uncoupled spins would also survive the z-filter.

Alternatively, one may also induce evolution of the AB spin system so that we may suppress it in an analogous way to what was shown above for the weakly-coupled spin system. For the case of strong coupling, the eigenstates are best approximated using the singlet-triplet basis [21, 22]:

$$|T_1\rangle = |\uparrow\uparrow\rangle$$

$$|T_0\rangle = \frac{1}{\sqrt{2}}(|\uparrow\downarrow\rangle + |\downarrow\uparrow\rangle)$$

$$|T_{-1}\rangle = |\downarrow\downarrow\rangle$$

$$|S_0\rangle = \frac{1}{\sqrt{2}}(|\uparrow\downarrow\rangle - |\downarrow\uparrow\rangle)$$

The three eigenstates $|T_1\rangle$, $|T_0\rangle$, and $|T_{-1}\rangle$ are referred to as triplet states, and $|S_0\rangle$ is called the singlet state. Importantly, the outer triplet states $|T_1\rangle$ and $|T_{-1}\rangle$ form a subspace when the Hamiltonian is written in this eigenbasis, as do the inner triplet $|T_0\rangle$ and singlet $|S_0\rangle$ states. Generating a population difference between the $|S_0\rangle$ and inner triplet $|T_0\rangle$ states, known as singlet order (SO), has attracted much attention in recent years because SO tends to decay much more slowly in certain nearly-symmetric molecules than longitudinal spin order between the outer triplet states $|T_1\rangle$ and $|T_{-1}\rangle$, which is governed by T_1 decay [21, 23].

SO, and in general what are known as long-lived states (LLS) [24], have been generated in various molecules between ^{1}H [23, 25, 26, 27], ^{13}C [28, 29], and ^{15}N [30, 31, 32] spins.

One pulse sequence element that has been used to produce SO is the J-synchronized spin echo train, used in the magnetization-to-singlet (M2S) and reverse (S2M) pulse sequences [30]. It can be shown that, by choosing the appropriate delay τ_{ET} on either side of each refocusing pulse and the number of spin echo blocks n_1 in the train, one can interconvert the singlet and inner triplet states while refocusing any evolution between the outer triplet states:

$$|T_0\rangle \xrightarrow{J-\text{syncET}} -ie^{i\frac{3\pi}{4}n_1}|S_0\rangle \tag{5}$$

$$|S_0\rangle \xrightarrow{J-\text{syncET}} -ie^{i\frac{3\pi}{4}n_1}|T_0\rangle$$

$$|T_1\rangle + |T_{-1}\rangle \xrightarrow{J-\text{syncET}} e^{-i\frac{5\pi}{4}n_1}\left(|T_1\rangle + |T_{-1}\rangle\right) \tag{6}$$

The parameters for the J-synchronized echo train can be calculated from the spin system parameters:

$$\tau_{ET} = \frac{\pi}{2\Omega_{AB}} \tag{7}$$

$$n_1 = \text{round}\left(\frac{\pi}{2\theta_{AB}}\right) \tag{8}$$

The expressions for Ω_{AB} and θ_{AB} are given above as Eqs. (3) and (4), respectively. The effectiveness of the J-synchronized echo train in interconverting the singlet and inner triplet states depends principally upon the mixing angle, θ_{AB}. Smaller mixing angles require more spin-echo blocks but can achieve a higher degree of interconversion, whereas larger mixing angles generally lead to a lower efficiency in singlet-triplet interconversion.

Consider the behavior of a strongly-coupled homonuclear spin system AB during a J-synchronized echo train following a broadband 90_y° excitation pulse. Such is the case following the first excitation pulse of the M2S pulse sequence. The spins are aligned along the x-axis following excitation, corresponding with

$$A_x + B_x = \frac{1}{\sqrt{2}}\left[\left(|T_1\rangle + |T_{-1}\rangle\right)\langle T_0| + |T_0\rangle\left(\langle T_1| + \langle T_{-1}|\right)\right]$$

in the singlet-triplet basis. Using Eqs. (5) and (6) and assuming perfect singlet-triplet interconversion, the new spin system state after the J-synchronized echo train is

$$\frac{i}{\sqrt{2}}\left[\left(|T_1\rangle + |T_{-1}\rangle\right)\langle S_0| - |S_0\rangle\left(\langle T_1| + \langle T_{-1}|\right)\right] = A_y - B_y$$

In converting back to the Cartesian basis, we discover that the two spins are now aligned anti-parallel to one another along the y-axis. This result is generalizable in that the J-synchronized spin echo train described above will always align the two strongly-coupled spins perpendicular to the axis they were previously aligned with, regardless of the phase of the initial excitation pulse.

We can now selectively spoil the signal arising from a strongly-coupled spin system AB, in a similar manner to that demonstrated above for a weakly-coupled spin system IS. Following broadband excitation, the J-synchronized spin echo train will induce a 90° phase shift in the

xy-plane in the AB system, whereas the IS spin system will evolve as described by Eqs. (1) and (2). After the J-synchronized spin-echo train (which has a total duration $2n_1\tau_{ET}$), the IS spin system will have evolved through an angle $\phi = 2\pi J_{IS} n_1 \tau_{ET}$. The next step, then, is to allow the IS spin system to evolve during a spin echo or echoes under $H_{J_{IS}}$ back to its original state following excitation. To prevent further evolution of the AB spin system, the new echo delay is chosen to be significantly different from that used in the J-synchronized spin echo train, or equivalence can be imposed upon the AB spins by radiofrequency (RF) pulsing (if the source of inequivalence is due to heteronuclear J-couplings, rather than a chemical shift difference). A z-filter can then be applied to attenuate the strongly-coupled spin system signal:

$$I_z{+}S_z{+}A_z{+}B_z \xrightarrow{90_y^\circ} I_x{+}S_x{+}A_x{+}B_x \xrightarrow{J-\text{syncET}} I_x\cos\phi{+}2I_yS_z\sin\phi{+}S_x\cos\phi{+}2I_zS_y\sin\phi{+}A_y{-}B_y$$

$$\xrightarrow{H_{J_{IS}}} I_x + S_x + A_y - B_y \xrightarrow{90_{-y}^\circ} I_z + S_z + A_y - B_y \xrightarrow{\text{spoil}} I_z + S_z$$

As with the other sequence, an excitation pulse and acquisition would measure the IS spin system signal. Note that, again, any uncoupled spins would survive the editing sequence and be detected in the resulting NMR spectrum.

The case of a strongly coupled chemically equivalent but magnetically inequivalent system can be described in complete analogy, since the M2S sequence has been shown to work there as well. For completeness, we note that other types of broadband triplet-to-singlet conversion sequences could also be used for this purpose [33].

3. Materials and Methods

3.1. Materials

β-nicotinamide adenine dinucleotide sodium salt (MW 685.41) and β-nicotinamide adenine dinucleotide hydrate reduced disodium salt hydrate (MW 709.40) were acquired from Sigma Aldrich. All samples included 50 mM each of NADH and NAD^+ and were prepared at room temperature. Every sample was dissolved in 900 uL of 50 mM TES buffer and 100 μL D_2O for locking and shimming purposes and pipetted into a Wilmad-LabGlass 5 mm high-throughput NMR tube.

3.2. NMR spectroscopy

NMR experiments were performed on a Bruker Avance NEO 400 MHz spectrometer with a 5mm Broadband Fluorine Observe Smart (BBFO) probe and with the temperature regulation set to 25 °C. Prior to each set of experiments, the probe was tuned and matched and the ^{31}P 90° pulse length was determined using the 360° zero-crossing. Unless otherwise noted, the NMR acquisition parameters used were the following: 2 s acquisition time, 7 s relaxation delay, 64 ms dwell time, 30720 complex points, 7.8 kHz spectral width, 8 scans.

Two ^{31}P NMR spectral editing sequences, described in greater detail in the Results section, were used to isolate either the NAD^+ or the NADH signal. Both sequences utilized spoiler gradients with duration 20 ms and 30% of maximum strength. All RF pulses and the receiver underwent a 4-step phase cycle. The sequence for isolating NAD^+ used composite 180° pulses with three 90-180-90 sub-pulses, as reported previously [34, 35]. The TopSpin "popt" routine

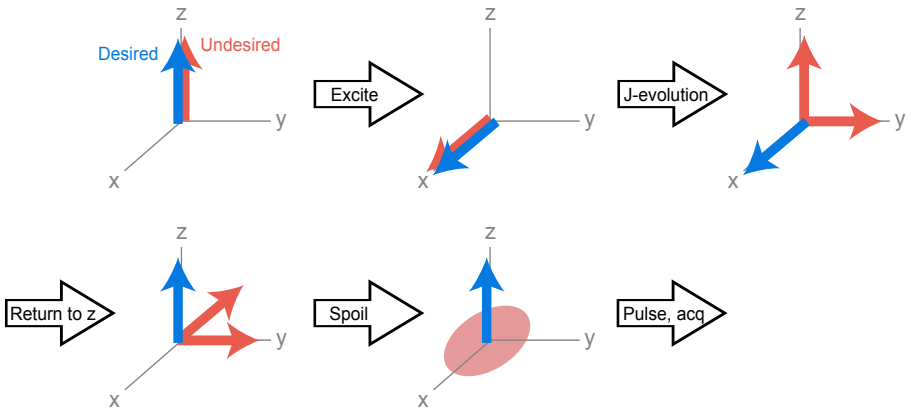

Figure 1: Schematic of the spectral editing approach. Magnetization arising from desired and undesired spins are separated from one another by selecting parameters that induce a 90° shift in the xy-plane due to J-coupling differences. The desired spin magnetization is then returned to the z-axis prior to spoiling the undesired spins. Finally, the desired spin magnetization is re-excited and measured.

was used for iterating parameter values during sequence optimization and robustness testing. For sequence optimization, timing and echo count parameters were optimized from earliest to latest in the pulse sequence, setting later delays close to zero while setting earlier delays to the optimized value.

3.3. Data analysis

The NMR spectra were analyzed in TopSpin. NADH and NAD^+ signals were quantified using integration. In the case of the pulse-sequence acquire spectrum, the downfield NAD^+ quadruplet peak overlaps significantly with NADH, making it difficult to isolate through integration. As a solution, the three upfield NAD^+ quadruplet peaks were integrated separately, and the integral of the upfield quadruplet peak was then multiplied by two. For spectra with edited sequences, each peak on the spectrum was quantified individually to determine the signals.

4. Results

We have designed two ^{31}P spectral editing pulse sequences to isolate either NAD^+ or NADH signals. The general approach, outlined in Fig. 1 and described in greater detail in the Theory section above, uses differences in J-coupling evolutions to place undesired spin magnetization perpendicular to the desired magnetization. A z-filter utilizing a 90° tip-back pulse with an appropriate phase returns the desired spin magnetization to the z-axis so that undesired signals can then be gradient-spoiled.

The J-selective z-filter technique lends itself well to the removal of spin systems that are weakly coupled, such as NAD^+. It would seem at first glance that NADH cannot be removed because it appears to give rise to a singlet peak in a ^{31}P NMR spectrum, suggesting that its two ^{31}P spins are equivalent and therefore will not evolve under J-coupling. This turns out not to be the case. ^{31}P NMR spectroscopy of an NADH sample using the spin-lock induced

coupling (SLIC) pulse sequence, which is able to populate and read out SO in strongly-coupled spin systems [36], shows signal derived from SO, indicating that the two ^{31}P in NADH are indeed inequivalent (Fig. S1A, Supplementary Material). Furthermore, applying ^{1}H decoupling on the 5' ribose methylene resonances during the spin-lock pulses removes the SO-derived signal (Fig. S1B, Supplementary Material). These findings confirm that the NADH ^{31}P nuclei are magnetically inequivalent due to the differences in J_{PH}-couplings of each ^{31}P nucleus with any one of the nearby methylene protons ($\Delta J_{\mathrm{PH}} \approx {}^{3}J_{\mathrm{PH}}$). We have observed the same phenomenon to occur in the molecule tetrabenzyl pyrophosphate [37], and others have seen the same between ^{13}C [28] and ^{15}N [32] spin pairs. By fitting the conventional ^{31}P NMR spectrum of NADH using the Spinach NMR simulation package in MATLAB [38], we obtained values for ${}^{2}J_{\mathrm{PP}}$ and ΔJ_{PH} that we used to simulate the behavior of the NAD$^+$ and NADH spins systems during our pulse sequences (Fig. S2, Supplementary Material). The homonuclear J-coupling is more than a factor of four greater than the inequivalence (i.e. $J_{PP} > 4 * {}^{3}J_{PH}$), meaning that NADH is strongly coupled and will not significantly evolve under $H_{J_{PP}}$. Additionally, our results suggest that ^{1}H decoupling on the 5' ribose methylene protons will impose equivalence upon the ^{31}P spins and prevent even minimal J-evolution (see Fig. S1B, Supplementary Material).

Our confirmation that ^{31}P SO could be accessed in NADH suggested that NMR singlet pulse sequence elements could be used to induce selective J_{PP}-evolution of NADH spins relative to NAD$^+$. As seen in the Theory section above, performing a spin-echo train with the echo time synchronized to the NADH J_{PP}-coupling can induce a 90° phase shift between NAD$^+$ and NADH spins. Combining these pulse sequence elements resulted in the spectral editing sequences shown in Fig. 2. Each sequence induces a 90° phase shift in either NAD$^+$ or NADH, then selectively removes the phase-shifted spin pair with either a single spin-echo or a spin-echo train. NADH J_{PP}-evolution is inhibited at various points in both sequences by 5' ribose methylene ^{1}H decoupling, which imposes equivalence on the NADH ^{31}P spins.

The optimized timing parameters for the two ^{31}P NMR spectral editing sequences are summarized in Table 1. The optimized values of the delays and echo numbers agree very well with results obtained by simulating the pulse sequences in Spinach, using the spin system parameters obtained from spectral fitting (Fig. S3, Supplementary Material).

Table 1: Optimized parameters for the ^{31}P spectral editing sequences, compared with values obtained by spin dynamics simulation.

Sequence	Parameter	Simulated value	Experimental optimization result
A	t_1	10.33 ms	10.6 ms
B	n_1	12-14 echoes	13 echoes
	t_1	12.4 ms	12.3 ms
	t_2	1 ms	1 ms

The performance of the ^{31}P NMR spectral editing sequences was initially assessed using a 1:1 NADH and NAD$^+$ sample on a 9.4 T NMR spectrometer. Fig. 3 displays a comparison of the resulting spectra from the two sequences with a conventional 90° pulse-acquire spectrum. The measured NAD$^+$/NADH ratio from the unedited spectra was 0.99. The spectral editing sequences exhibited high selectivity, with both sequences significantly attenuating the undesired metabolite's signal relative to the desired metabolite (Table 2). Using both edited

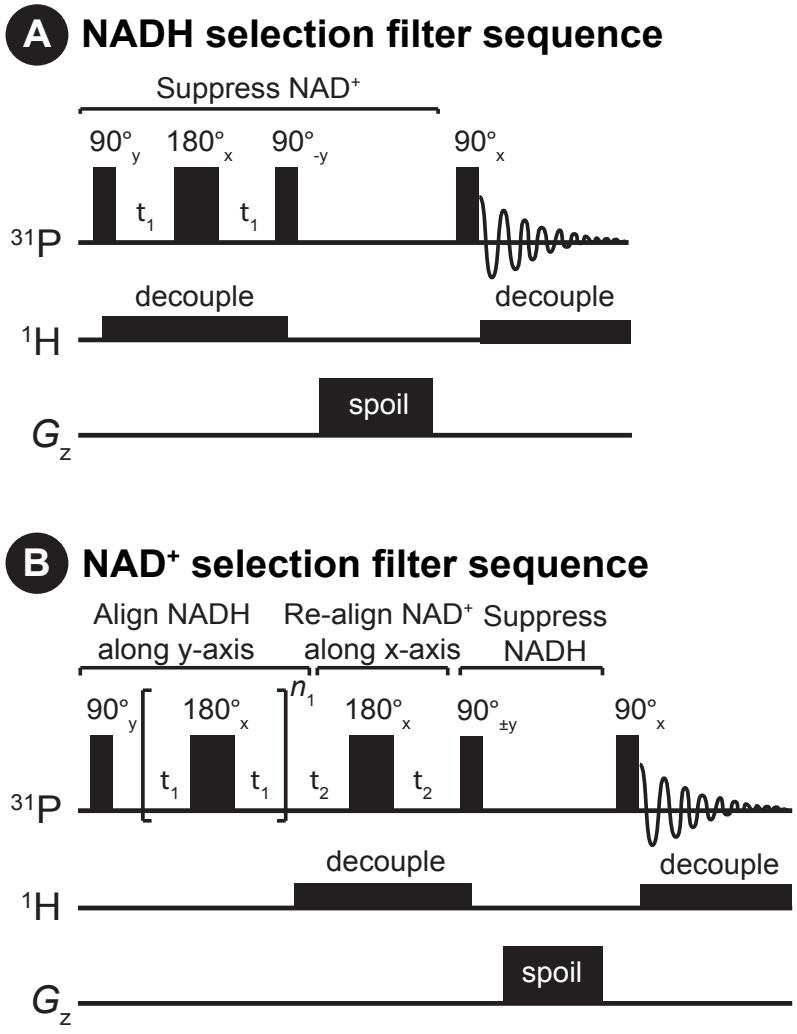

Figure 2: Pulse sequence diagrams for ^{31}P NMR spectral editing sequences, to isolate either NADH (**A**, top) or NAD$^+$ (**B**, bottom). Four-step phase cycling on all pulses is not shown.

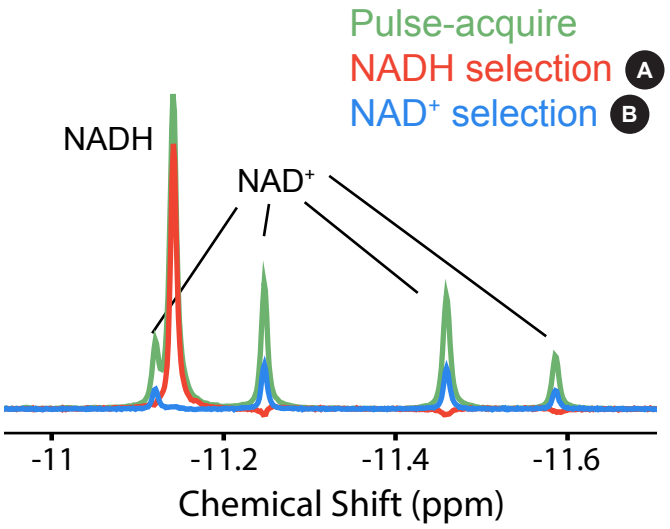

Figure 3: Comparison of ^{31}P NMR spectra obtained from a sample of 1:1 NADH:NAD$^+$ using the two pulse sequences shown in Fig. 2, compared with a pulse-acquire spectrum. ^{1}H decoupling was applied at the 5'-ribose methylene proton frequency during acquisition.

spectra, the measured NAD$^+$/NADH ratio is 0.43. The NADH selection sequence reduced the NADH by 24.4% and the NAD$^+$ selection sequence reduced the NAD$^+$ by 66.9%. These signal reductions appear to be primarily due to T_2 decay between the excitation and tipback pulses, since the desired NMR signal from each spectral editing sequence and a TR-matched perfect echo sequence are similar in magnitude (Fig. S4, Supplementary Material).

Table 2: Signal attenuation of the undesired and desired metabolites signals with the edited sequences, relative to the signal from a pulse-acquire NMR spectrum.

Sequence	Undesired Signal Attenuation %	Desired Signal Attenuation %
A	95.8	23.4
B	99.1	66.9

The NAD spectral editing sequences were then evaluated in terms of their robustness to imperfections in B_0 and pulse frequency offset, which pose challenges for most spectral editing techniques. The results are displayed in Fig. 4. Increasing B_0 inhomogeneity by approximately 15 Hz via misset shims does not significantly affect the measured NAD$^+$/NADH ratio (Fig. 4A); the measured ratio from the broadened spectra is 0.41, which is only 4.7% lower than that with good shimming. Both spectral editing sequences also demonstrate good robustness to transmitter offset (Fig. 4B-C). The NADH selection sequence keeps the undesired NAD$^+$ $< 10\%$ of the NADH signal within the offset frequency range of ± 2000 Hz, while the NAD$^+$ selection sequence keeps the undesired NADH signal $< 20\%$ of NAD$^+$ within ± 1000 Hz (Fig. 4D-E).

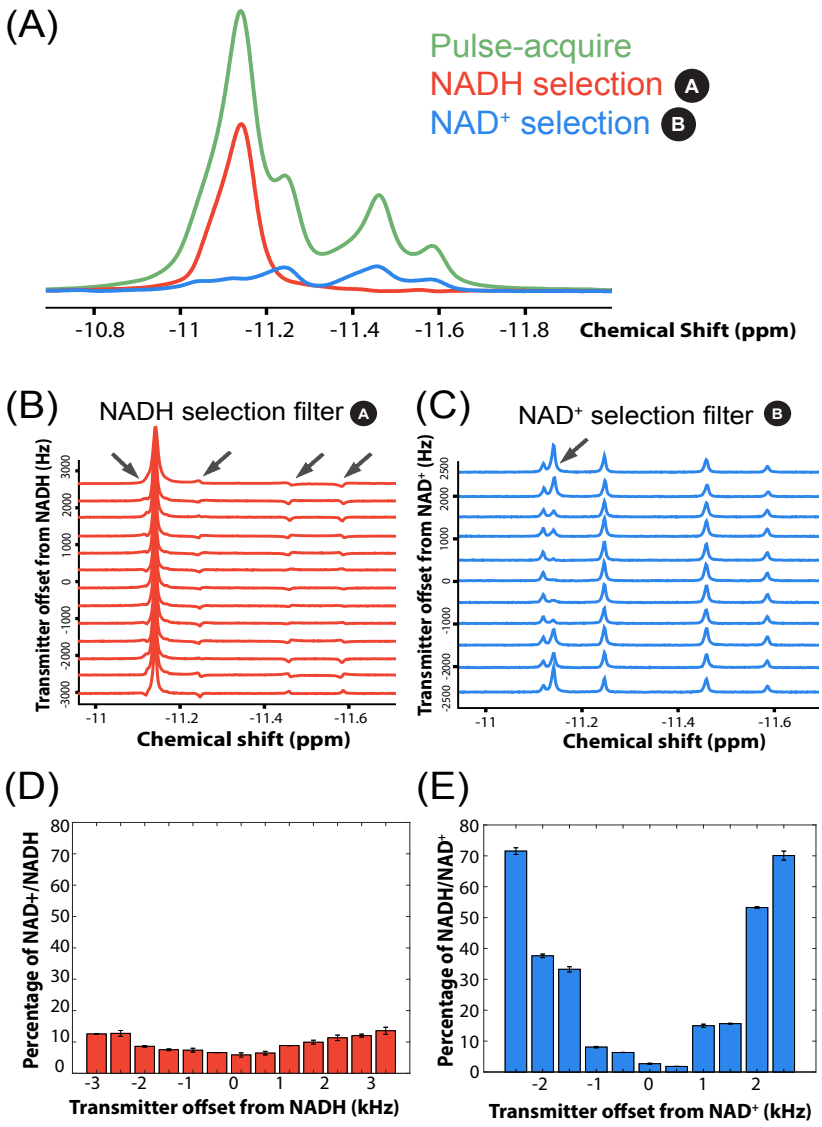

Figure 4: Robustness of ^{31}P spectral editing sequences to B_0 inhomogeneity and transmitter offset. (A) NMR spectra obtained after inducing ~15 Hz of spectral line broadening by missetting shims. (B-C) NMR spectra acquired while adjusting transmitter offset relative to the NADH ^{31}P peak for the (B) NADH selection sequence; and (C) NAD^+ selection sequence, with black arrows indicating the undesired NAD^+ or NADH signals. (D-E) the absolute integral ratio of the undesired metabolite to the desired metabolite in the edited spectrum for each sequence, measured as a function of transmitter offset. The sample for all figure parts contained 1:1 NAD^+:NADH.

5. Discussion

This study presents ^{31}P NMR spectral editing pulse sequences to isolate either NAD$^+$ or NADH from the mixture of them. We make use of the fact that the two ^{31}P spins within NAD$^+$ and NADH are in different J-coupling regimes at 9.4 T to selectively isolate and suppress one or the other. The z-filter technique returns the desired spin magnetization to the z-axis, whereas the undesired spins are spoiled in the xy-plane. A similar approach to the weakly-coupled spin removal sequence has been reported by Jayasundar *et al.*, for spectral editing of ^{31}P NMR of blood [39]. In this work, 2,3-diphosphoglycerate was efficiently removed by allowing the heteronuclear ^{1}H-^{31}P J-coupling to evolve, then converting it into either multiple-quantum coherences, two-spin order, or a ^{1}H-detectable coherence. Similarly, our developed sequence for removal of weakly-coupled ^{31}P spins, in our case those in NAD$^+$, works in a straightforward manner. In contrast, NADH appears to give rise to a singlet peak in a ^{31}P NMR spectrum, which suggests that its two ^{31}P spins are strongly coupled and therefore do not evolve under J-coupling in the same way as for NAD$^+$. However, we discovered that NADH can sustain SO due to the inequivalence between ^{31}P spins arising from heteronuclear couplings. DeVience *et al.* had earlier characterized SO between the ^{31}P nuclei in NAD$^+$, but not NADH, at 4.7 T [40]. We therefore turned to a singlet-triplet description of the NADH ^{31}P spins, and we discovered that a pulse sequence element developed for SO population and readout, the J-synchronized echo train, could help us selectively remove the NADH signal. The J-synchronized echo train has also been implemented recently for performing 1D and 2D J-spectroscopy at 6.5 mT [41]. Our optimized pulse sequence parameters agree well with those predicted using NMR simulations and the spin system parameters obtained from spectral fitting. In addition, the performance and the robustness of the two ^{31}P spectral editing sequences were tested with respect to offset and B_0 inhomogeneity. The spectral editing sequences exhibited high selectivity, with both sequences strongly attenuating the undesired metabolite relative to the desired one. The two spectral editing sequences also showed their robustness to imperfections in B_0, which pose challenges for most spectral editing techniques. The NADH selection filter is more robust to the transmitter offsets than the NAD$^+$ selection filter, which makes sense based upon the fewer number of RF pulses. The transmitter offset robustness of the NAD$^+$ selection filter could perhaps be improved by using a different composite 180° pulse with a higher pulse offset tolerance, such as a $90_x240_y90_x$ or a $90_x225_{-x}315_x$ composite pulse [42, 43].

Other spectral editing approaches have been developed that select signals with an associated NMR singlet state, removing other signals from the resulting spectrum. Early on, DeVience *et al.* proposed the Suppression of Undesired Chemicals using Contrast-Enhancing Singlet States (SUCCESS) pulse sequence, which tunes the RF offset and delay parameters to prepare SO in a desired spin pair, preserve it under spin locking for a delay period, then reconvert it to detectable magnetization, filtering out undesired resonances in the process [44]. They first showed good selection of aspartate, threonine, and glutamate ^{1}H pairs over other metabolites *in vitro* [44], then later they showed they could remove adenosine triphosphate (ATP) signal while retaining NAD$^+$ and adenosine diphosphate (ADP) in ^{31}P NMR spectra [40]. Drawbacks include a strong dependence on RF transmitter frequency, and thus sensitivity to B_0 inhomogeneity, and the need for spin locking to preserve SO for high signal, increasing power deposition into the sample or subject. Kiryutin *et al.* developed the

Singlet Order Selection (SOS) filter [45], which prepares and detects SO while effectively suppressing residual background signals using adiabatically-ramped RF fields, known as the Adiabatic-Passage Spin Order Conversion (APSOC) sequence [46]. They showed excellent isolation of ^{1}H resonances from both strongly- and weakly-coupled spin systems in polypeptides and small proteins by tuning the RF offset and maximum RF amplitude based upon the spin system parameters. Similar to the SUCCESS sequence, the strong dependence of the editing efficiency upon the RF offset frequency may cause problems if the main field is very inhomogeneous. Xin *et al.* reported an approach to isolate glutamate (Glu) or glutamine (Gln) ^{1}H signals using optimal control to design metabolite-specific RF pulses that transfer magnetization to and from SO as a filtration method [47]. Their results at 11.7 T highlighted their ability to selectively isolate either Glu or Gln while suppressing other signals, and they demonstrated *in vivo* Glu and Gln selection in a healthy human brain on a 3 T clinical scanner. Their simulation data suggested that B_0 and transmit field (B_1) inhomogeneity significantly decreased the efficiency of resonance isolation, although the authors proposed designing broadband pulses with their optimal control approach to mitigate B_0 effects. Mamone *et al.* demonstrated a more robust approach by generalizing the M2S-S2M sequence to a general coupling M2S (gcM2S) method for spectral editing [48]. They also showed its applicability to specifically detect important brain metabolites in *ex vivo* tissue and amyloid-beta residues by choosing timing parameters corresponding with the desired spin system, which can fall within a wide range of coupling regimes. Like our NADH sequence, the gcM2S uses a J-synchronized spin-echo train for strongly-coupled spin systems. Unlike the gcM2S, our sequence does not fully populate SO but stops halfway through the process, potentially speeding up the sequence while still benefitting from the advantages of using broadband RF pulses. It is worth noting that, unlike singlet state filtration methods, our NADH-type pulse sequence cannot directly remove non-coupled spins in the form reported in this manuscript. However, by taking the sequence and changing the $90_{\pm y}$ pulse to a 90_{x} pulse (see Fig. 2, sequence **B**), we would align the strongly-coupled spin system along the z-axis. By doing so, we could spoil other types of spin systems, including isolated spins with no J-coupling. The two strongly-coupled spins would then be re-excited and undergo another J-synchronized echo train to align them parallel rather than antiparallel for detection. We have not yet tested this pulse sequence modification, but presumably it would feature a shorter sequence time than equivalent J-synchronized echo sequences for singlet-filtered NMR.

We show specifically for NAD^+ and NADH that it is possible to isolate both resonances from one another with the sequences we developed. The results could be used in studies that aim to investigate metabolism and the roles of NAD^+ and NADH in various biological processes. *In vivo* experiments with the edited sequences may be challenging at high field strengths because of the short T_2 values of the metabolites (e.g. 8-19 ms in the human brain on a 9.4 T scanner [49]), but lower field strengths may benefit from longer ^{31}P T_2 values. Assuming the ^{31}P T_2 is dominated by chemical shift anisotropy, studies at 3 T would be expected to have T_2 values of 79-187 ms, which would limit signal loss and lead to higher sensitivity. However, this would also reduce the chemical shift dispersion between NAD^+ ^{31}P peaks and push it toward an intermediately coupled regime. Another challenge for NAD^+ and NADH quantification with our pulse sequences is the large α-ATP resonance *in vivo*, which is typically an order of magnitude higher than NAD and resonates at a similar chemical shift. We have performed preliminary studies which show that α-ATP can be

attenuated by adding a perfect echo module [50] to the spectral editing sequences reported herein (data not shown). One possible scenario where ^{31}P NAD spectral editing may be useful is in NMR experiments of living cells, perfused tissue samples, or cell/tissue extracts, where quantification of ATP, intracellular pH, and other metabolites can inform on cell metabolic changes [51, 52, 53, 54, 55, 56].

Although our first demonstration of this approach to spectral editing was applied to ^{31}P NMR spectroscopy, we expect that it will also be applicable to editing ^{1}H spectra as well. Metabolites that have previously been the target of J-difference spectral editing, including GABA, lactate, GSH, and 2HG, have weakly-coupled spins at clinical MRI field strengths and could be removed selectively from ^{1}H spectra using an NAD^{+}-type sequence. There may be other metabolites which have strongly coupled pairs of ^{1}H nuclei that could be edited out with an NADH-type sequence to improve quantification of other metabolites. One possible target is citrate, which has protons in the strongly-coupled regime and therefore has been shown to sustain long-lived states [26]. As shown for the gcM2S filtration sequence, NAA and the collective glutamine-glutamate (Glx) peaks could also be isolated or selectively suppressed [48]. A difference approach could also be conceived of to obtain the NMR spectrum of a single metabolite, in which case a difference spectrum between edited and unedited spectra would isolate the desired resonance.

6. Conclusions

In conclusion, we have developed two ^{31}P NMR spectral editing pulse sequences that allow for the selective detection of either NAD^{+} or NADH. By utilizing differences in J-coupling regimes and a z-filter technique, we were able to isolate the desired spin magnetization and suppress undesired signals. Our findings suggest that NADH experiences a two-bond J-coupling and an inequivalence arising from the difference in J_{PH}-couplings of each ^{31}P nucleus with nearby methylene protons. We confirmed that NMR singlet pulse sequence elements can induce selective J_{PP}-evolution of NADH spins relative to NAD^{+}. The resulting spectral editing sequences demonstrated high selectivity, and their optimized timing parameters agreed very well with NMR simulation data. The NAD spectral editing sequences were also found to be robust to imperfections in B_0 and pulse frequency offset. Hence, these results provide a valuable tool for studying the roles of NAD^{+} and NADH in cellular metabolism and energy production. The spectral editing approach shown in our work is general and could be applied to simplify the spectra of other NMR-active nuclei, including for ^{1}H spectroscopy.

7. Acknowledgments

AJ acknowledges funding through an award from the US National Science Foundation, award no. CHE 2108205 and an award from the Heising-Simons Foundation.

Conflicts of interest

There are no conflicts to declare.

References

[1] A. Bax, L. Lerner, Two-dimensional nuclear magnetic resonance spectroscopy, Science 232 (4753) (1986) 960–967.

[2] H. Kessler, M. Gehrke, C. Griesinger, Two-dimensional NMR spectroscopy: Background and overview of the experiments [new analytical methods (36)], Angewandte Chemie International Edition in English 27 (4) (1988) 490–536.

[3] H. Y. Carr, E. M. Purcell, Effects of diffusion on free precession in nuclear magnetic resonance experiments, Physical review 94 (3) (1954) 630.

[4] S. Meiboom, D. Gill, Modified spin-echo method for measuring nuclear relaxation times, Review of scientific instruments 29 (8) (1958) 688–691.

[5] J. V. Hajnal, B. De Coene, P. D. Lewis, C. J. Baudouin, F. M. Cowan, J. M. Pennock, I. R. Young, G. M. Bydder, High signal regions in normal white matter shown by heavily T_2 weighted CSF nulled IR sequences, J Comput Assist Tomogr 16 (4) (1992) 506–513.

[6] J.-B. Hövener, D. J. Rigotti, M. Amann, S. Liu, J. S. Babb, P. Bachert, A. Gass, R. I. Grossman, O. Gonen, Whole-brain N-acetylaspartate MR spectroscopic quantification: Performance comparison of metabolite versus lipid nulling, American Journal of Neuroradiology 29 (8) (2008) 1441–1445.

[7] W. Bogner, G. Hangel, M. Esmaeili, O. C. Andronesi, 1D-spectral editing and 2D multispectral *in vivo* ^{1}H-MRS and ^{1}H-MRSI-methods and applications, Analytical biochemistry 529 (2017) 48–64.

[8] I.-Y. Choi, O. C. Andronesi, P. Barker, W. Bogner, R. A. Edden, L. G. Kaiser, P. Lee, M. Marjańska, M. Terpstra, R. A. de Graaf, Spectral editing in ^{1}H magnetic resonance spectroscopy: Experts' consensus recommendations, NMR in Biomedicine 34 (5) (2021) e4411.

[9] A. Jenne, W. Bermel, C. A. Michal, O. Gruschke, R. Soong, R. Ghosh Biswas, M. Bastawrous, A. J. Simpson, Dreamtime NMR spectroscopy: Targeted multicompound selection with improved detection limits, Angewandte Chemie International Edition 61 (19) (2022) e202110044.

[10] J. A. Aguilar, P. I. P. Elliott, J. López-Serrano, R. W. Adams, S. B. Duckett, Only para-hydrogen spectroscopy (OPSY), a technique for the selective observation of para-hydrogen enhanced NMR signals, Chemical Communications (11) (2007) 1183–1185.

[11] J. A. Aguilar, R. W. Adams, S. B. Duckett, G. G. R. Green, R. Kandiah, Selective detection of hyperpolarized NMR signals derived from para-hydrogen using the Only Para-hydrogen SpectroscopY (OPSY) approach, Journal of Magnetic Resonance 208 (1) (2011) 49–57.

[12] A. N. Pravdivtsev, V. P. Kozinenko, J.-B. Hövener, Only Para-Hydrogen Spectroscopy (OPSY) Revisited: In-Phase Spectra for Chemical Analysis and Imaging, The Journal of Physical Chemistry A 122 (45) (2018) 8948–8956.

[13] A. N. Pravdivtsev, F. Sönnichsen, J.-B. Hövener, OnlyParahydrogen SpectrosopY (OPSY) pulse sequences – One does not fit all, Journal of Magnetic Resonance 297 (2018) 86–95.

[14] N. Mueller, R. R. Ernst, W. Kurt, Multiple-quantum-filtered two-dimensional correlated NMR spectroscopy of proteins, Journal of the American Chemical Society 108 (21) (1986) 6482–6492.

[15] O. Sørensen, M. Rance, R. Ernst, z Filters for purging phase-or multiplet-distorted spectra, Journal of Magnetic Resonance (1969) 56 (3) (1984) 527–534.

[16] M. G. Vander Heiden, R. J. DeBerardinis, Understanding the intersections between metabolism and cancer biology, Cell 168 (4) (2017) 657–669.

[17] M. Lu, X.-H. Zhu, Y. Zhang, W. Chen, Intracellular redox state revealed by *in vivo* ^{31}P MRS measurement of NAD^+ and NADH contents in brains, Magnetic resonance in medicine 71 (6) (2014) 1959–1972.

[18] R. A. de Graaf, H. M. De Feyter, P. B. Brown, T. W. Nixon, D. L. Rothman, K. L. Behar, Detection of cerebral NAD^+ in humans at 7 T, Magnetic resonance in medicine 78 (3) (2017) 828–835.

[19] J. Ren, C. R. Malloy, A. D. Sherry, Quantitative measurement of redox state in human brain by ^{31}P MRS at 7 T with spectral simplification and inclusion of multiple nucleotide sugar components in data analysis, Magnetic resonance in medicine 84 (5) (2020) 2338–2351.

[20] T. Nakai, C. A. Mcdowell, INADEQUATE NMR spectra of extremely strongly coupled spin systems, Molecular Physics 79 (5) (1993) 965–983.

[21] M. H. Levitt, Singlet nuclear magnetic resonance, Annual review of physical chemistry 63 (2012) 89–105.

[22] G. Pileio, Singlet NMR methodology in two-spin-1/2 systems, Progress in nuclear magnetic resonance spectroscopy 98 (2017) 1–19.

[23] M. Carravetta, O. G. Johannessen, M. H. Levitt, Beyond the T_1 limit: Singlet nuclear spin states in low magnetic fields, Physical Review Letters 92 (15) (2004) 153003.

[24] F. Teleanu, A. Sadet, P. R. Vasos, Symmetry versus entropy: Long-lived states and coherences, Progress in Nuclear Magnetic Resonance Spectroscopy 122 (2021) 63–75.

[25] M. S. Anwar, D. Blazina, H. A. Carteret, S. B. Duckett, T. K. Halstead, J. A. Jones, C. M. Kozak, R. J. K. Taylor, Preparing High Purity Initial States for Nuclear Magnetic Resonance Quantum Computing, Physical Review Letters 93 (4) (2004) 040501.

[26] G. Pileio, M. Concistrè, M. Carravetta, M. H. Levitt, Long-lived nuclear spin states in the solution NMR of four-spin systems, Journal of Magnetic Resonance 182 (2) (2006) 353–357.

[27] N. M. Ariyasingha, O. G. Salnikov, K. V. Kovtunov, L. M. Kovtunova, V. I. Bukhtiyarov, B. M. Goodson, M. S. Rosen, I. V. Koptyug, J. G. Gelovani, E. Y. Chekmenev, Relaxation dynamics of nuclear long-lived spin states in propane and propane-d6 hyperpolarized by parahydrogen, The Journal of Physical Chemistry C 123 (18) (2019) 11734–11744.

[28] Y. Feng, R. Davis, W. Warren, Accessing long-lived nuclear singlet states between chemically equivalent spins without breaking symmetry, Nature physics 8 (11) (2012) 831–837.

[29] G. Stevanato, J. T. Hill-Cousins, P. Håkansson, S. S. Roy, L. J. Brown, R. C. D. Brown, G. Pileio, M. H. Levitt, A nuclear singlet lifetime of more than one hour in room-temperature solution, Angewandte Chemie International Edition 54 (12) (2015) 3740–3743.

[30] G. Pileio, M. Carravetta, M. H. Levitt, Storage of nuclear magnetization as long-lived singlet order in low magnetic field, Proceedings of the National Academy of Sciences 107 (40) (2010) 17135–17139.

[31] R. V. Shchepin, J. R. Birchall, N. V. Chukanov, K. V. Kovtunov, I. V. Koptyug, T. Theis, W. S. Warren, J. G. Gelovani, B. M. Goodson, S. Shokouhi, M. S. Rosen, Y.-F. Yen, W. Pham, E. Y. Chekmenev, Hyperpolarizing concentrated metronidazole $^{15}NO_2$ group over six chemical bonds with more than 15 % polarization and a 20 minute lifetime, Chemistry – A European Journal 25 (37) (2019) 8829–8836.

[32] K. Sheberstov, H. Vieth, H. Zimmermann, B. Rodin, K. Ivanov, A. Kiryutin, A. Yurkovskaya, Generating and sustaining long-lived spin states in (15)N,(15)N'-azobenzene, Science reports 9 (1) (2019) 20161.

[33] C. Bengs, M. Sabba, A. Jerschow, M. H. Levitt, Generalised magnetisation-to-singlet-order transfer in nuclear magnetic resonance, Physical Chemistry Chemical Physics 22 (17) (2020) 9703–9712.

[34] M. H. Levitt, Symmetrical composite pulse sequences for NMR population inversion. I. compensation of radiofrequency field inhomogeneity, Journal of Magnetic Resonance (1969) 48 (2) (1982) 234–264.

[35] M. C. Tayler, M. H. Levitt, Singlet nuclear magnetic resonance of nearly-equivalent spins, Physical Chemistry Chemical Physics 13 (13) (2011) 5556–5560.

[36] S. J. DeVience, R. L. Walsworth, M. S. Rosen, Preparation of nuclear spin singlet states using spin-lock induced crossing, Physical review letters 111 (17) (2013) 173002.

[37] D. E. Korenchan, J. Lu, M. H. Levitt, A. Jerschow, ^{31}P nuclear spin singlet lifetimes in a system with switchable magnetic inequivalence: Experiment and simulation, Physical Chemistry Chemical Physics 23 (35) (2021) 19465–19471.

[38] H. J. Hogben, M. Krzystyniak, G. T. Charnock, P. J. Hore, I. Kuprov, Spinach–a software library for simulation of spin dynamics in large spin systems, Journal of Magnetic Resonance 208 (2) (2011) 179–194.

[39] R. Jayasundar, T. J. Norwood, L. D. Hall, N. M. Bleehen, Spectral editing techniques for ^{31}P NMR spectroscopy of blood, Magnetic Resonance in Medicine 10 (1) (1989) 89–95.

[40] S. J. DeVience, R. L. Walsworth, M. S. Rosen, NMR of 31P nuclear spin singlet states in organic diphosphates, Journal of Magnetic Resonance 333 (2021) 107101.

[41] S. J. DeVience, M. S. Rosen, Homonuclear J-coupling spectroscopy using J-synchronized echo detection, Journal of Magnetic Resonance 341 (2022) 107244.

[42] M. H. Levitt, Composite pulses, Progress in Nuclear Magnetic Resonance Spectroscopy 18 (2) (1986) 61–122.

[43] M. H. Levitt, Composite Pulses, in: R. K. Harris (Ed.), Encyclopedia of Magnetic Resonance, John Wiley & Sons, Ltd, Chichester, UK, 2007, pp. 1396–1411.

[44] S. J. DeVience, R. L. Walsworth, M. S. Rosen, Nuclear spin singlet states as a contrast mechanism for NMR spectroscopy, NMR in Biomedicine 26 (10) (2013) 1204–1212.

[45] A. S. Kiryutin, A. N. Pravdivtsev, A. V. Yurkovskaya, H.-M. Vieth, K. L. Ivanov, Nuclear spin singlet order selection by adiabatically ramped RF fields, The Journal of Physical Chemistry B 120 (46) (2016) 11978–11986.

[46] A. N. Pravdivtsev, A. S. Kiryutin, A. V. Yurkovskaya, H.-M. Vieth, K. L. Ivanov, Robust conversion of singlet spin order in coupled spin-1/2 pairs by adiabatically ramped RF-fields, Journal of Magnetic Resonance 273 (2016) 56–64.

[47] J.-X. Xin, D.-X. Wei, Y. Ren, J.-L. Wang, G. Yang, H. Zhang, J. Li, C. Fu, Y.-F. Yao, Distinguishing glutamate and glutamine in in vivo 1H MRS based on nuclear spin singlet order filtering, Magnetic Resonance in Medicine 89 (5) (2023) 1728–1740.

[48] S. Mamone, N. Rezaei-Ghaleh, F. Opazo, C. Griesinger, S. Glöggler, Singlet-filtered NMR spectroscopy, Science Advances 6 (8) (2020) eaaz1955.

[49] J. Dorst, T. Borbath, L. Ruhm, A. Henning, Phosphorus transversal relaxation times and metabolite concentrations in the human brain at 9.4 T, NMR in Biomedicine 35 (10) (2022) e4776.

[50] J. A. Aguilar, M. Nilsson, G. Bodenhausen, G. A. Morris, Spin echo NMR spectra without J modulation, Chem Commun (Camb) 48 (6) (2012) 811–3.

[51] T. O. Henderson, A. J. R. Costello, A. Omachi, Phosphate metabolism in intact human erythrocytes: Determination by phosphorus-31 nuclear magnetic resonance spectroscopy, Proceedings of the National Academy of Sciences of the United States of America 71 (6) (1974) 2487–2490.

[52] R. J. Gillies, K. Ugurbil, J. A. den Hollander, R. G. Shulman, ^{31}P NMR studies of intracellular pH and phosphate metabolism during cell division cycle of saccharomyces cerevisiae., Proceedings of the National Academy of Sciences of the United States of America 78 (4) (1981) 2125–2129.

[53] P. Meneses, T. Glonek, High resolution ^{31}P NMR of extracted phospholipids, Journal of Lipid Research 29 (5) (1988) 679–689.

[54] K. R. Keshari, J. Kurhanewicz, R. E. Jeffries, D. M. Wilson, B. J. Dewar, M. Van Criekinge, M. Zierhut, D. B. Vigneron, J. M. Macdonald, Hyperpolarized ^{13}C spectroscopy and an NMR-compatible bioreactor system for the investigation of real-time cellular metabolism, Magnetic Resonance in Medicine 63 (2) (2010) 322–329.

[55] K. R. Keshari, R. Sriram, M. Van Criekinge, D. M. Wilson, Z. J. Wang, D. B. Vigneron, D. M. Peehl, J. Kurhanewicz, Metabolic reprogramming and validation of hyperpolarized ^{13}C lactate as a prostate cancer biomarker using a human prostate tissue slice culture bioreactor, The Prostate 73 (11) (2013) 1171–1181.

[56] Y. Liu, Y. Gu, X. Yu, Assessing tissue metabolism by phosphorous-31 magnetic resonance spectroscopy and imaging: A methodology review, Quantitative Imaging in Medicine and Surgery 7 (6) (2017) 707–726.